

# Chapter 4

## Multi-axis Capability for Powered Ankle-Foot Prostheses

Evandro M. Ficanha, Mohammad Rastgaar, and Kenton R. Kaufman

**Abstract** The ankle joint of lower extremity powered prostheses are generally designed to be capable of controlling a single degree of freedom (DOF) in the sagittal plane, allowing a focus on improved mobility in straight walking. However, the single DOF ankle movements are rare in normal lower limb actions such as walking on a straight path or turning when the ankle movements in both sagittal and frontal planes are significant. Therefore, the effectiveness of next-generation lower extremity prostheses may be significantly enhanced by improved understanding of the ankle dynamics in both sagittal and frontal planes during different maneuvers and by implementing strategies to account for these intricacies in prosthesis design.

In this chapter, the concept of a multi-axis powered ankle-foot prosthesis is introduced. The feasibility of this concept, to the extent allowed, by a proof of concept prototype is shown. Further, the design kinematics and its mechanical impedance in non-load bearing conditions are evaluated and discussed. It is shown that the proposed cable-driven mechanism for the multi-axis powered ankle-foot prosthesis is capable of closely mimicking the ankle movements in both sagittal and frontal planes during step turn and walking on straight path.

**Keywords** Multi-axis ankle-foot prosthesis • Powered lower extremity prosthesis • Human ankle impedance • Cable-driven prosthesis

---

E.M. Ficanha • M. Rastgaar (✉)  
Department of Mechanical Engineering-Engineering Mechanics, Michigan Technological University, Houghton, MI 49931, USA  
e-mail: [Rastgaar@mtu.edu](mailto:Rastgaar@mtu.edu)

K.R. Kaufman  
Motion Analysis Laboratory, Department of Orthopedic Surgery, Mayo Clinic and Mayo Foundation, Rochester, MN 55905, USA

## 4.1 Introduction

Recent advances in powered prostheses promise to significantly improve the quality of life and well-being for individuals with impaired mobility. A majority of people without disabilities, 61.4 % to be exact, report their health to be excellent. In sharp contrast, only 28.4 % of people with disabilities report the same. Moreover, people with disabilities are at a greater risk for secondary conditions (e.g., injury, obesity, and hypertension) that can further impact well-being and diminish overall quality of life [1]. A better understanding of the complexities surrounding lower limb prostheses, which are needed for walking and daily activity will lead to increased health and well-being for the 1.7 million limb amputees in the US, the majority of whom have lower extremity amputations [2, 3]. The ankle joint of lower extremity powered prostheses currently commercially available is capable of controlling only one degree of freedom (DOF) in the sagittal plane, allowing a focus on improved mobility in straight walking. Turning, however, plays a major role in daily living activities and requires ankle torque in both sagittal and frontal planes. Therefore, the effectiveness of next-generation lower extremity prostheses may be significantly enhanced by improved understanding of ankle dynamics in both sagittal and frontal planes during different maneuvers and by implementing strategies to account for these intricacies in prosthesis design.

A multi-axis ankle-foot prosthetic robot capable of generating torques in both the sagittal and frontal planes with impedance modulation similar to the human ankle may improve maneuverability and increase mobility. It is shown that unilateral below-knee amputees who use passive prostheses rely more on their hip joint and expend 20–30 % more metabolic energy compared to non-amputees at the same speed. As a result, their preferred speed of gait is 30–40 % lower than non-amputees [4, 5] and their compensatory gait strategies results in asymmetrical gait patterns that affect joints in both lower limbs [6–9]. Net positive work generated in the ankle contributes to propulsion in gait. It has been shown that a powered ankle-foot prosthesis reduces the metabolic costs of unilateral transtibial amputees during straight walking by providing sufficient power during push-off [10, 11]. However, studies of four representative daily activities show that turning steps may account for an average of 25 % of steps, ranging from 8 to 50 % of all steps depending on the activity [12], which amputees accomplish using different gait strategies than non-amputees. While a non-amputee relies on the hip movement in the coronal plane and moment generated in the ankle joint, an amputee using a passive prosthesis relies on hip extension in the sagittal plane [13–16]. During a turn, modulation of ankle impedance in sagittal and frontal planes plays a major role in controlling lateral and propulsive ground reaction forces in order to accelerate the body center of mass along the gait path; thus, during a step turn, lateral and propulsive impulses are larger compared to a straight step [17]. This difference will result in different gait strategies between amputees and non-amputees to compensate for the lack of propulsion in the passive prostheses to increase maneuverability [13]. This suggests that an ankle-foot prosthesis controllable in two planes, i.e. dorsiflexion-plantarflexion (DP)

and inversion-eversion (IE) directions, may increase the mobility by providing more assistance in turning. Additionally, designing a feature that allows walking in arbitrary directions on slopes while conforming the foot to the ground profile and uneven surfaces may result in a more efficient gait.

Passive lower extremity prostheses do not store or generate energy. Understanding of the ankle's capability in impedance modulation and generating net positive work during the stance period of gait has influenced the design of new ankle-foot prostheses [18–21]. One design approach is based on storing energy during the heel strike and releasing it during the push-off before the trailing foot's heel strike. Collins and Kuo [22] developed a microprocessor-controlled artificial foot that limits the increase in metabolic cost to 14 % compared to 23 % that occurs with a passive prosthesis. The positive work by the prosthesis at the push-off partially compensates for the dissipative negative work at the heel strike of the trailing foot and lowers the redirection of the body's center of mass velocity [23–27]. On the other hand, there are powered prostheses capable of injecting energy to the system. Klute et al. developed a prototype using McKibben pneumatic actuators [28]. Sup et al. developed a powered transfemoral prosthesis with active knee and ankle joints, each with one controllable DOF in the sagittal plane [29–32]. The controller adjusts the impedance at a number of instants during gait by altering the neutral position of the ankle. Hitt et al. designed an ankle-foot prosthesis using a lightweight robotic tendon actuator that provided the majority of peak power for push-off [33, 34]. Au et al. developed an ankle-foot prosthesis [35–37] that later transitioned into a commercially available ankle-foot prosthesis, BiOM [38]. An adaptive muscle-reflex controller for this powered prosthesis was developed further by Eilenberg et al. using an ankle plantar-flexor model based on a Hill-type muscle and a positive force feedback reflex. A finite state machine determined the phase of the gait; hence, the appropriate ankle torques [39]. The controller in the BiOM allows for gait with different cadence over surfaces with different inclinations, e.g. uphill and downhill trajectories [40]. Other commercially available powered transtibial prostheses are the Proprio foot from össur and the Elan from Endolite; however neither provides a net positive work during the stance period [41, 42]. BiOM provides the necessary energy during toe-off and generates a net positive work [43, 10] that has been shown to reduce the metabolic costs by 8.9–12.1 % at different gait speeds compared to a passive prosthesis. The improvements occurred for gait speeds between 1 and 1.75 m/s; however, it did not change the metabolic cost at 0.75 m/s, suggesting a possible optimal range of speed for its design [44]. The BiOM also increased the preferred gait speed by 23 % [44] and lowered loading of the intact leg during level-ground walking, which may lower the risk of secondary complications [45].

Because the ankle is a biomechanically complex joint with multiple DOFs, failure to incorporate full function of the ankle into prostheses design can inadvertently lead to secondary complications [46]. Mechanical impedance of a dynamic system determines the evoked torque to the motion perturbations and is a function of the stiffness, visco-elasticity, and inertia of the system. Ankle mechanical impedance in no load-bearing conditions has been studied in the sagittal plane [47–61].

Quasi-static ankle stiffness in both DP and IE were reported by Roy et al. [62], but coupling between these DOFs was not assessed. The ankle impedance during load-bearing conditions has also been studied. In the frontal plane, Saripalli et al. [63] studied the variation of ankle stiffness under different load-bearing conditions. Zinder et al. [64] studied dynamic stabilization and ankle stiffness in IE by applying a sudden perturbation in the frontal plane during bipedal weight-bearing stance. In the sagittal plane, the quasi-stiffness of the ankle has been studied and suggests humans change their reflex ankle stiffness in response to unpredicted perturbations [65]. Loram et al. determined that the intrinsic ankle stiffness during a quiet stance is almost constant with respect to ankle torque and suggested that the central nervous system contributes to the balance by modulating ankle stiffness especially with the triceps surae muscles in the sagittal plane [66, 67]. Sasagawa et al. made a similar conclusion with subjects standing on inclined surfaces moving forward and backward [68]. Ankle quasi-static stiffness was studied during quiet standing [69, 70] and locomotion [18, 20, 71]. Variations of ankle moment, ankle angle, and speed dependent hysteresis during gait cycles at different speeds was studied by Hansen et al. [21]. Also, dynamic stiffness of lower limbs during hopping and running was measured by Farley et al. [72, 73]. Recently, Rouse et al. developed a perturbation platform to estimate ankle impedance during the foot-flat phase of the stance period of gait in the DP direction [74–76].

The ankle's mechanical impedance in a single degree of freedom has been the focus of the studies in all of the prior work and the multidirectional characteristics of the ankle has not been addressed. The ankle joint is biomechanically complex and consists of multiple degrees of freedom. It's major anatomical axes are non-orthogonal with no intersection that could introduce a biomechanical coupling between DP and IE. Additionally, single DOF ankle movements are rare in normal lower limb actions and the control of multiple ankle DOFs presents unique challenges [77]. Therefore, understanding the directional impedance of the ankle requires a multivariable identification approach. Multivariable mechanical impedance of the human ankle in both DP and IE directions in stationary conditions was estimated by Rastgaar et al. [78, 79] for dynamic mechanical impedance and Lee et al. [80–83] for quasi-static mechanical impedance. Ho et al. also studied the directional variation of quasi-static mechanical impedance of ankle [84, 85]. Further, Lee et al. developed a method for estimation of time-varying mechanical impedance of the ankle during the entire stride length for the subjects walking on a treadmill [86]. Their study on ten unimpaired subjects showed consistent time-varying characteristics of ankle impedance during the entire stride in both sagittal and frontal planes.

In this chapter, we introduced the concept of a multi-axis powered ankle-foot prosthesis and showed the feasibility of this concept to the extent allowed by a proof of concept prototype. We first described the experiments for collecting the information on the range of motion (ROM) of the ankle during step turn and walking on straight path in both sagittal and frontal planes. The ankle displacements need to be studied since the mechanical impedance of the ankle is a dynamic operator that maps the time-history of angular displacements onto the corresponding time-history

of torques at the ankle joint. Next, the design of the proof of concept prototype of a steerable ankle-foot prosthesis will be explained. Further, the design kinematics and its mechanical impedance in non-load bearing conditions will be evaluated and discussed.

## 4.2 Ankle Rotations During the Step Turns and Straight Steps

Straight walking requires a complex sequence of muscle activation to modulate the ground reaction forces to produce forward motion. Similarly, modulation of the reaction forces is required for turning the body [13]. Two different strategies that are commonly used for turning are the spin turn and the step turn. The spin turn consists of turning the body around the leading leg (e.g. turning right with the right leg in front). The step turn consists of shifting the body weight to the leading leg and stepping onto the opposite leg while still shifting the body weight (e.g. turning left with the right leg in front). The step turn is more stable since the base of support for body weight is wider [15] and for this reason it was used in this study. It has been shown that the step turn velocity, length, and width are considerably different than the straight walk with higher turning reaction forces [17]. Three-dimensional measurement of the ankle angles during step and spin turns have been previously studied [87]; however, it is of interest to study the ankle angular displacements during different phases of the stance period during step turns and comparing these results to the ankle angles during straight steps. Additionally, the collected data were used to evaluate the kinematic design of the ankle-foot prototype in reproducing the same trajectories. This will be discussed later in this chapter. Different approaches have been used to measure ankle angles such as using flexible electro-goniometer, electromagnetic tracking devices, and motion capturing cameras [14, 87, 17, 15, 88]. We used a motion capture camera system to track the three-dimensional rotations of the foot and tibia in stance periods during two gait scenarios: 1- walking on a straight path and 2-90 degree step turn.

The motion capture camera system consisted of eight cameras in a square formation covering a volume of about 16 cubic meters and an area of 12 square meters. The cameras emitted infrared light and captured the reflected light from reflectors mounted on the participants with a rate of 250 Hz. Five male subjects with no self-reported neuromuscular and biomechanical disorders were recruited for the experiments. The subjects gave written consent to participate in the experiment that was approved by the Michigan Technological University Institutional Review Board.

The subjects were instructed to walk at a normal pace and an audible metronome was synchronized to their number of steps per minute in an attempt to keep the walking speed constant. The preferred speed for the participants ranged from 88 to 96 steps per minute. They started walking from outside the field of view of the cameras while following a straight line marked on the floor. When they reached a reference point on the floor, they performed a 90° step turn to the left, pivoting on

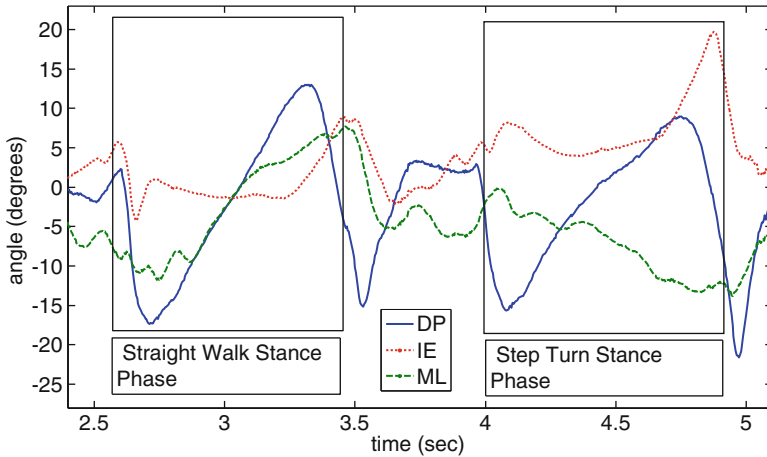


**Fig. 4.1** A representative subject’s ankle rotations in DP, IE, and ML directions during the straight walk and step turn

their right leg and continued walking straight until they were outside the field of view of the cameras. Each subject repeated the test nine times, after several training trials to increase the consistency of the trials. Time trajectories of the markers on the tibia and foot were used to estimate the ankle rotations.

The plots of DP, IE, and medial/lateral (ML) angles for a representative subject are shown in Fig. 4.1. The data for each test was divided into 6 phases (heel strike, flat foot, and toe-off for both straight and turning steps) and the averages of the DP, IE, and ML rotations of each phase were calculated for all 9 trials of 5 subjects (a total of 45 trials).

Table 4.1 shows the average ROM of the subjects during the straight step and step turn stance periods. The maximum and minimum angles and maximum angular velocities observed for the representative subject in Fig. 4.1 can also be seen in Table 4.1. Table 4.2 shows the average rotations and the difference in angles from the turning step to the straight step in each phase. The range of motion of each subject’s ankle about the three axes of the ankle and their average rotations during the stance periods were calculated and used to find the averaged percent change from straight walk to step turn with respect to their ROM during the straight step (Table 4.2).

The duration of the combined phases of heel strike and loading response, mid stance, and terminal stance and pre-swing phases were determined and used to measure the average angles at each combined phase.

There was a modest decrease of ROM in DP direction during the step turn compared to the straight step. ROM in the IE direction increased by 23.8 % indicating the significance of the IE role during turning. A significantly smaller range of motion in ML may suggest a higher stiffness in that axis of rotation necessary to transfer the reaction forces from the ground to the body.

**Table 4.1** ROM of ankle during the stance in straight walk and step turn

|    | ROM of straight step stance period (deg) |                | ROM of step turn stance period (deg) |                |          |                            |                            |                                       |
|----|------------------------------------------|----------------|--------------------------------------|----------------|----------|----------------------------|----------------------------|---------------------------------------|
|    | Degrees                                  | Standard error | Degrees                              | Standard error | % Change | Maximum angle <sup>a</sup> | Minimum angle <sup>a</sup> | Maximum angular velocity <sup>a</sup> |
| DP | 33.9                                     | 0.65           | 31.6                                 | 0.62           | -7.4     | 13.03°                     | -21.58°                    | 120°/s                                |
| IE | 15.69                                    | 0.52           | 20.6                                 | 1.06           | 23.8     | 19.72°                     | -4.248°                    | 101°/s                                |
| ML | 22.09                                    | 0.6            | 16.8                                 | 0.65           | -31.9    | 7.69°                      | -13.75°                    | 144°/s                                |

<sup>a</sup>Representative subject

**Table 4.2** Average angles at different phases of stance in straight step and step turn

|                | Straight step average (deg) | Standard error | Turning step average (deg) | Standard error | Angular change (deg) <sup>a</sup> | % Change <sup>b</sup> |
|----------------|-----------------------------|----------------|----------------------------|----------------|-----------------------------------|-----------------------|
| DP heel Strike | -8.72                       | 0.80           | -9.68                      | 0.95           | -0.95                             | -3.0                  |
| DP flat foot   | 2.34                        | 0.63           | 0.36                       | 0.64           | -1.98                             | -6.5                  |
| DP toe off     | 10.59                       | 1.24           | 1.37                       | 0.90           | -9.22                             | -29.2                 |
| IE heel strike | -1.72                       | 0.53           | 5.90                       | 0.63           | 7.61                              | 46.6                  |
| IE flat foot   | -2.93                       | 0.27           | 6.51                       | 0.22           | 9.44                              | 60.5                  |
| IE toe off     | 1.44                        | 0.45           | 13.61                      | 0.46           | 12.17                             | 82.0                  |
| ML heel strike | -5.34                       | 0.57           | 0.34                       | 0.62           | 5.68                              | 25.6                  |
| ML flat foot   | -0.90                       | 0.45           | -3.55                      | 0.41           | -2.65                             | -12.8                 |
| ML toe off     | 5.53                        | 0.32           | -6.53                      | 0.65           | -12.06                            | -58.0                 |

<sup>a</sup>Turning step angles – Straight step angles

<sup>b</sup>From straight to step turn with respect to individual straight walk ROM in stance period

As the step progressed through the gait cycle, noticeable differences were observed between the straight step and step turn for all subjects. DP displacement started at a similar initial angle as the straight step at the heel strike ( $-9.68^\circ$  of dorsiflexion) but progressively showed less plantarflexion at toe-off ( $1.37^\circ$  in step turn compared to  $10.37^\circ$  in straight walk). IE displacement started with  $5.9^\circ$  of inversion at heel strike and increased to  $13.6^\circ$  at toe-off during the step turn suggesting a gradual increase in inversion to lean the body toward the inside of the turn. At the heel strike of the step turn, ML displacement had an increase of  $5.68^\circ$  of medial rotation compared to straight walk that may suggest an anticipatory motion of the foot. The difference in lateral rotation during straight step and step turn at the toe-off increased to  $12.06^\circ$ .

### 4.3 Multi-axis Ankle-Foot Prototype

The result from the ankle rotations in three DOF suggested that a multi-axis mechanism in a prosthesis may enhance gait efficiency by adding control of ankle inversion/eversion during turning. This novel design is anticipated to enable the device to adapt to uneven and inclined ground surface condition and allow the amputees to benefit more from their prosthesis rather than using their hip joint; enabling a more natural gait with less stress in other joints.

Based on this concept, a prototype cable-driven ankle-foot prosthesis with two controllable degrees of freedom (Fig. 4.2) was designed to evaluate the feasibility of controlling a 2 DOF ankle joint. The design goals were to meet the ROM and angular velocity required for straight walk and step turn while providing sufficient torque for propulsion.

The device consisted of a pylon (A), two DC motors (E) and planetary gearheads (D) that are powered by two motor controllers (B) that receive signals from a DAQ

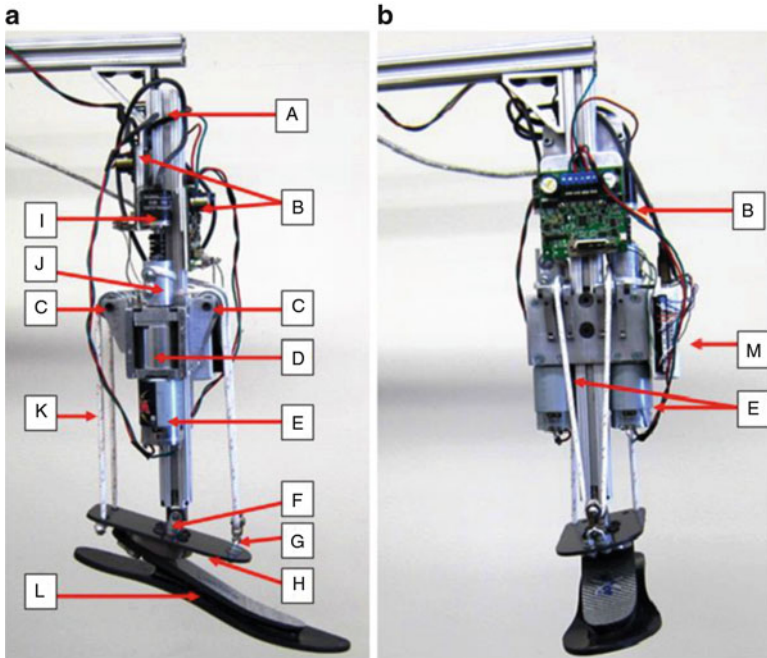


**Fig. 4.2** Prototype of a multi-axis powered ankle-foot prosthesis (a) in plantarflexion and (b) in inversion

board (M) connected to a remote computer and two quadrature encoders (I). Two cable drums (J) transfer the required torque to the ankle through a nylon rope (K) that passes through two pulleys (C). The rope is looped around both the cable drums and secured to prevent slippage (Fig. 4.3). A universal joint (F) connects the pylon to the foot and an elastic carbon-fiber plate. The rope is attached to a carbon fiber plate (H) that is connected to a commercially available prosthetic foot (Otto Bock Axtion<sup>®</sup>) (L). In the aft side of the carbon fiber plate, the rope is mounted at both sides of the longitudinal axes of the foot. At the fore side, the rope passes through a pulley (G) that is connected to the carbon fiber plate by a universal joint. The mechanism is capable of both dorsiflexion-plantarflexion when the motors rotate in opposite directions and inversion-eversion when the motors rotate in the same direction. Also, any combination of DP and IE can be achieved by combining different amounts of rotations at each motor.

The proposed design with two controllable DOFs relies on the fact that three points are sufficient to define a plane in the space. As shown in Fig. 4.4, the three points (A, B, C) can be used to define rotations of the foot relative to the pylon about the X and Y axes that are equivalent to DP and IE, respectively. If the motors apply forces in the same directions, for example in the negative Y direction, points A and B will move downwards, while point C moves upwards, resulting in dorsiflexion. If the motors move in opposite directions, for example the right motor pull the rope

**Fig. 4.3** Cable drum connection to avoid cable slippage

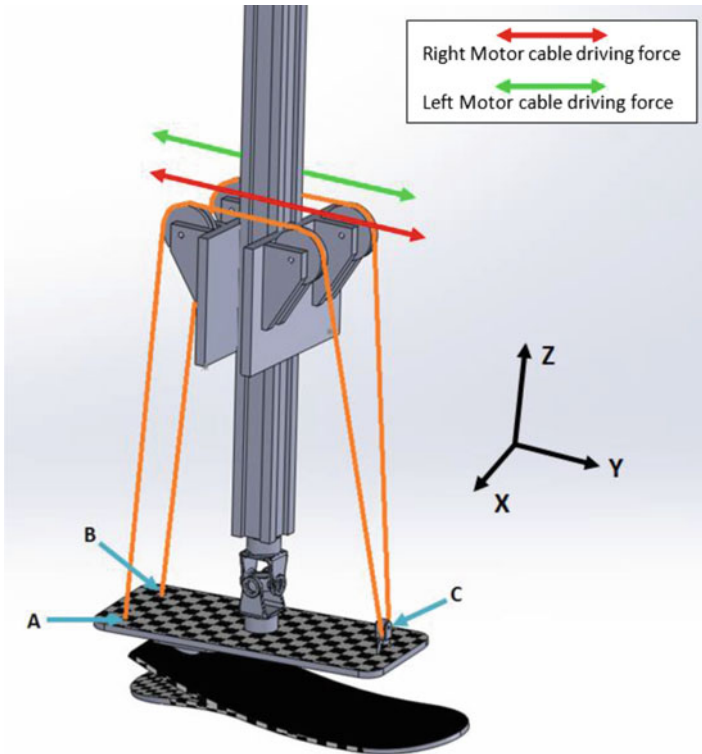


**Fig. 4.4** A simplified drawing of the cable driven mechanism showing three interaction points A, B, and C between the cable, carbon fiber plate, and motor drive forces

in the positive Y direction and the left motor pulls the rope in negative Y direction, point A moves upwards, while point B moves downwards generating foot eversion. At point C, a pulley is mounted to the plate using a universal joint. Because point C is located on the axis of symmetry of the plate and the rope passes through the pulley at point C, no DP motion is generated. The carbon fiber plate is a fundamental component of the design. The carbon fiber plate acts as a spring element in series with the cable and the foot. The cable needs to be always in tension to assure proper control over the foot and keep the carbon fiber plate under a bending moment. This assures the cable has a sufficient tension over the ROM of the foot providing that it can be controlled to mimic the mechanical impedance of a human ankle.

Providing sufficient power and torque at the ankle joint without significant increase in the weight of the powered prostheses is a challenging issue. For example, Hitt et al. used two parallel actuators to increase the power output for walking in increased speed [33]. The steering mechanism proposed here also use two actuators; however, the design allows for generating a torque component in lateral plane. The cable driven design, besides the ability to control the ankle in two DOF, may provide a significant flexibility in managing the inertia of the ankle-foot prostheses too. A detailed description of the components used in this proof of concept prototype can be found in [89].

## 4.4 Evaluation of the Design Concept

The developed prototype has been evaluated for meeting two criteria. First, the design kinematics should be capable of regenerating the same ankle rotation as the human ankle during the stance and swing phases of gait. Second, the multivariable impedance of the prototype ankle needs to be comparable to the mechanical impedance of human ankle.

### 4.4.1 Kinematic Evaluation

Presently, two optical quadrature encoders (200 pulses per revolution) provide position feedback to a remote computer that uses a proportional plus rate controller to control the relative position of the foot with respect to the pylon. The controller uses a look-up table with recorded angles of the representative subject of the motion analysis experiment in both DP and IE. The input and output angles to the controller can be seen in Fig. 4.5 where the robot is moving at 50 % of the walking speed. For ease of comparison, the output plots have a time shift to remove the 80 milliseconds delay of the output. Also, all signals are filtered with a low-pass filter with a cutoff frequency of 5 Hz to remove sensor noise from the output signal. The current prototype was developed as a proof of concept to validate the design kinematics; therefore, faster motors and sensors with lower noise levels will be used in future designs.

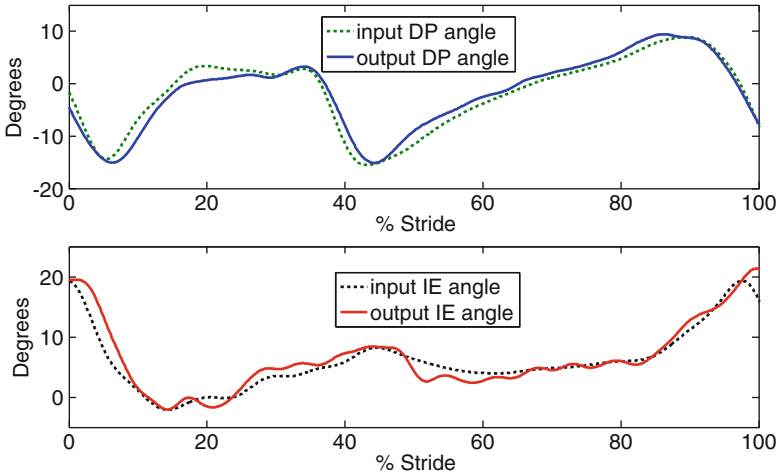


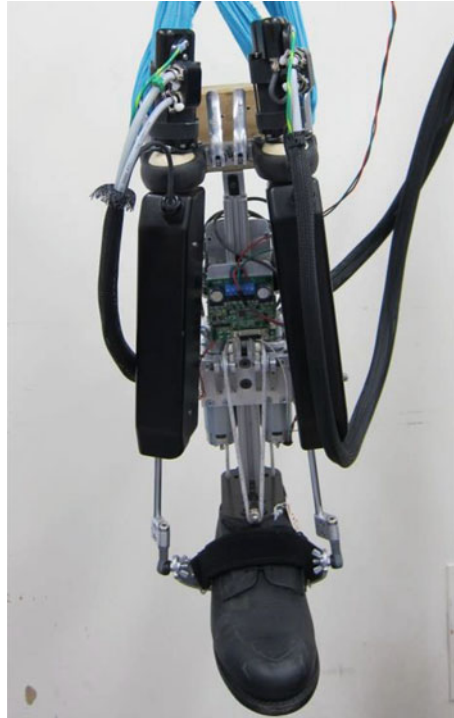
**Fig. 4.5** Input and compensated output for time delay (80 ms) of the ankle-foot prosthesis during swing and stance periods of a step turn at 50 % of the walking speed with no load

#### 4.4.2 Mechanical Impedance Estimation

Recently, hierarchical control strategies have been developed for impedance control of active prostheses [39, 30]. The higher level control identifies the gait cycle, and the lower level control regulates the actuators for a proper impedance characteristics. Following the same strategies, an ankle-foot prosthesis can be designed to have an initial mechanical impedance similar to a human's ankle. This may provide a faster modulation of the ankle impedance based on the state of the gait cycle.

The purpose of this evaluation was to identify the passive impedance of the prosthetic device and compare it to the impedance of human subjects. The impedance estimation experiment setup was similar to the procedure reported in [79, 78], where an Anklebot<sup>®</sup> was used to apply random torque perturbations to the ankle joint in DP and IE directions with a bandwidth of 100 Hz and record the provoked ankle angles. A stochastic system identification method was used to estimate the multivariable mechanical impedance of the ankle using the collected data. Similar procedures were used for estimation of passive mechanical impedance of the ankle-foot prosthesis while all its controllers were turned off. The experimental setup can be seen in Fig. 4.6, where the two devices were attached mechanically to each other. The Otto Bock Axtion<sup>®</sup> foot and its rubber foot shell were inserted in the same type of shoe used in human tests to ensure consistency in the experiments. Similarly, the same test was done on a representative human subject for comparison with the prosthesis. Impedance test of the human subject was performed with both relaxed muscles and 10 % MVC of the tibialis anterior following the procedures described in [79]. The EMG signals were monitored using a Delsys Trigno Wireless EMG System<sup>®</sup> with surface electrodes placed at the belly of the tibialis anterior. The EMG

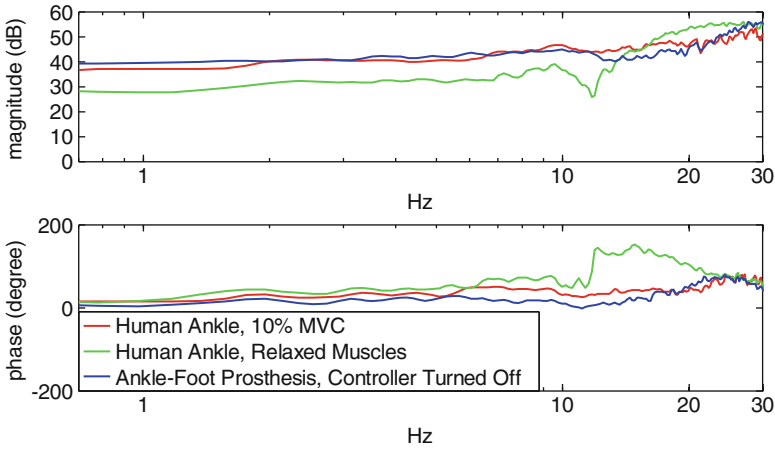
**Fig. 4.6** Anklebot attached to the prosthetic foot to measure the mechanical impedance of the ankle-foot prosthesis



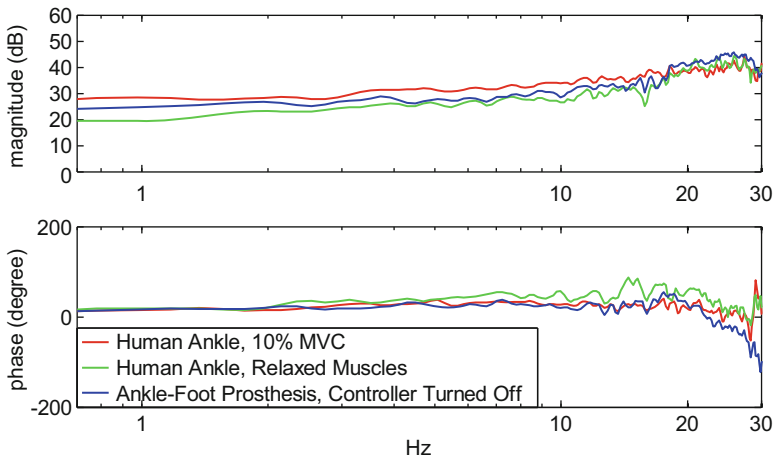
signal was sampled at 2 kHz and the root-mean-square value of a window of 13.5 ms of data calculated and displayed on a computer screen in order to provide a visual feedback to the participant for maintaining constant muscle activity. The results can be seen in Figs. 4.7 and 4.8.

Figure 4.7 shows the Bode plots of the mechanical impedances in DP direction for prototype prosthesis, human subject's ankle with relaxed muscles, and human subject's ankle with 10 % MVC. The quasi-static stiffness of the prototype prosthesis, which is the impedance magnitude at low frequencies, was 39.5 dB (94 N.m/deg) in DP at 1 HZ. Also, it shows a relatively linear impedance and phase over the frequency range of interest (0–5 HZ). The human subject showed similar stiffness in DP for the co-contraction testes and lower stiffness in passive test when compared to the prosthesis. IE impedance magnitude (Fig. 4.8) of the prosthesis was between the active and passive stiffness of the human sample with a value of 24.24 dB (16 N.m/deg) at 1 Hz.

While the maximum lifting force of the robot in the z axis was generated, the carbon fiber plate flexed due to the applied torque. Since the encoders read the cable displacement instead of foot angles, the controller perceived the deflection of the carbon fiber plate as an angular displacement of the foot. This caused the position controller to reduce the torque being applied prematurely, and thus the maximum lifting force was less than anticipated, although it was still powerful enough to lift a



**Fig. 4.7** Plots of the magnitude and phase of the impedance in DP rotation of the prosthetic robot and a human subject with relaxed muscles and 10 % cocontraction



**Fig. 4.8** Plots of the magnitude and phase of the impedance in IE rotation of the prosthetic robot and a human sample with relaxed muscles and 10 % cocontraction

72 KG person. Future designs will benefit from position sensors which can measure the foot angles directly to increase the precision of the position and the resulting torque.

Testing the range of motion in IE, it was found that the IE motion might become unstable when exceeds 62 degrees due to an external force. This is the equivalent of rolling the ankle, which is a common injury among active people and are mostly in inversion [63]. From the gait analysis experiment, it was seen that the maximum rotation in IE (Table 4.1) was 19.72°, and thus instability should not impose a significant issue during normal gait.

The current developments in control strategies for prostheses suggests that the control of the ankle joint in the ankle-foot prosthesis should mimic the time-varying impedance of the ankle in two DOF during different phases of stance period in different gait scenarios while providing the required torque. Recent work by Lee et al. and Rouse et al. [76, 86] are notable for estimating the time-varying ankle impedance during both swing and stance periods of gait along a straight path. To estimate the time-varying impedance of the ankle during a turning maneuver, a perturbing walkway may be necessary. The implemented mechanical design, although in early stages of development, showed anthropomorphic characteristics. The design was successful at mimicking human motion, and showed mechanical impedance similar to human ankle.

## References

1. Health and Wellness for Persons with Disabilities Today (2007) Office of the Surgeon General <https://www.ncbi.nlm.nih.gov/books/NBK44662/>
2. A Roadmap for US Robotics, From Internet to Robotics: Computing Community Consortium (2013) <http://www.us-robotics.us/reports/CCC%20Report.pdf>.
3. Ziegler-Graham K, MacKenzie EJ, Ephraim PL, Travison TG, Brookmeyer R (2008) Estimating the prevalence of limb loss in the United States: 2005 to 2050. *Arch Phys Med Rehabil* 89(3):422–429
4. Colborne GR, Naumann S, Longmuir PE, Berbrayer D (1992) Analysis of mechanical and metabolic factors in the gait of congenital below knee amputees. *Am J Phys Med Rehabil* 92:272–278
5. Molen NH (1973) Energy/speed relation of below-knee amputees walking on motor-driven treadmill. *Internationale Zeitschrift für angewandte Physiologie einschließlich Arbeitsphysiologie* 31(3):173–185
6. Winter DA, Sienko SE (1988) Biomechanics of below-knee amputee gait. *J Biomech* 21(5):361–367
7. Skinner HB, Effeney DJ (1985) Gait analysis in amputees. *Am J Phys Med Rehabil* 64:82–89
8. Bateni H, Olney S (2002) Kinematic and kinetic variations of below-knee amputee gait. *J Prosthet Orthot* 14(1):2–13
9. Adamczyk PG, Kuo AD (2011) Asymmetry in Amputee Gait: the propagating effects of weak push-off. In: American Society of Biomechanics, Long Beach, CA
10. Herr HM, Grabowski AM (2010) Powered ankle-foot prosthesis improves metabolic demand of unilateral transtibial amputees during walking. In: American Society of Biomechanics, Long Beach, CA
11. Ferris AE, Aldridge JE, Sturdy JT, Wilken JM (2011) Evaluation of the biomimetic properties of a new powered ankle-foot prosthetic system. American Society of Biomechanics, Long Beach, CA
12. Glaister BC, Bernatz GC, Klute GK, Orendurff MS (2007) Video task analysis of turning during activities of daily living. *Gait Posture* 25(2):289–294
13. Ventura JD, Segal AD, Klute GK, Neptune RR (2011) Compensatory mechanisms of transtibial amputees during circular turning. *Gait Posture* 34:307–312
14. Orendurff MS, Segal AD, Berge JS, Flick KC, Spanier D, Klute GK (2006) The kinematics and kinetics of turning: limb asymmetries associated with walking a circular path. *Gait Posture* 23(1):106–111
15. Hase K, Stein RB (1999) Turning strategies during human walking. *J Neurophysiol* 81(6):2914–2922

16. Segal AD, Orendurff MS, Czerniecki JM, Schoen J, Klute GK (2011) Comparison of transtibial amputee and non-amputee biomechanics during a common turning task. *Gait Posture* 33(1):41–47. doi:[10.1016/j.gaitpost.2010.09.021](https://doi.org/10.1016/j.gaitpost.2010.09.021)
17. Glaister BC, Orendurff MS, Schoen JA, Bernatz GC, Klute GK (2008) Ground reaction forces and impulses during a transient turning maneuver. *J Biomech* 41(4):3090–3093
18. Palmer M (2002) Sagittal plane characterization of normal human ankle function across a range of walking gait speeds. Massachusetts Institute of Technology, Cambridge, MA
19. Gates DH (2004) Characterizing ankle function during stair ascent, descent, and level walking for ankle prosthesis and orthosis design. Boston University, Boston
20. Davis R, DeLuca P (1996) Gait characterization via dynamic joint stiffness. *Gait Posture* 4(3):224–231
21. Hansena AH, Childress DS, Miff SC, Gard SA, Mesplay KP (2004) The human ankle during walking: implications for design of biomimetic ankle prostheses. *J Biomech* 37:1467–1474
22. Collins SH, Kuo AD (2010) Recycling energy to restore impaired ankle function during human walking. *PLoS One* 5(2)
23. Donelan JM, Kram R, Kuo AD (2002) Mechanical work for step-to-step transitions is a major determinant of the metabolic cost of human walking. *J Exp Biol* 205:3717–3727
24. Donelan JM, Kram R, Kuo AD (2002) Simultaneous positive and negative external work in human walking. *J Biomech* 35:117–124
25. Ruina A, Bertram JE, Srinivasan M (2005) A collisional model of the energetic cost of support work qualitatively explains leg sequencing in walking and galloping, pseudoelastic leg behavior in running and the walk-to-run transition. *J Theor Biol* 237(2):170–192
26. Kuo AD (2002) Energetics of actively powered locomotion using the simplest walking model. *J Biomech Eng* 124:113–120
27. Kuo AD, Donelan JM, Ruina A (2005) Energetic consequences of walking like an inverted pendulum: step-to-step transitions. *Exerc Sport Sci Rev* 33:88–97
28. Klute GK, Czerniecki J, Hannaford B (1998) Development of powered prosthetic lower limb. In: Proceedings of the 1st national meeting, Veterans Affairs Rehabilitation Research and Development Service, Washington, D.C.
29. Goldfarb M (2010) Powered robotic legs – leaping toward the future. National Institute of Biomedical Imaging and Bioengineering. <http://www.nibib.nih.gov/news-events/newsroom/powered-robotic-legs-leaping-toward-future>
30. Sup F, Bohara A, Goldfarb M (2008) Design and control of a powered transfemoral prosthesis. *Int J Robot Res* 27:263–273
31. Sup F, Varol HA, Mitchell J, Withrow TJ, Goldfarb M (2009) Preliminary evaluations of a self-contained anthropomorphic transfemoral prosthesis. *IEEE ASME Trans Mechatron* 14(6):667–676
32. Iv FCS (2009) A powered self-contained knee and ankle prosthesis for near normal gait in transfemoral amputees. Vanderbilt University, Nashville
33. Hitt J, Merlo J, Johnston J, Holgate M, Boehler A, Hollander K, Sugar T (2010) Bionic running for unilateral transtibial military amputees. In: 27th Army Science Conference (ASC), Orlando, Florida
34. Hitt JK, Sugar TG, Holgate M, Bellman R (2010) An active foot-ankle prosthesis with biomechanical energy regeneration. *J Med Devices* 4(1):011003
35. Au SK (2007) Powered ankle-foot prosthesis for the improvement of amputee walking economy. Massachusetts Institute of Technology, Cambridge, MA
36. Au S, Herr H (2008) Powered ankle-foot prosthesis. *Robot Autom Mag* 15(3):52–59
37. Au S, Weber J, Herr H (2009) Powered ankle-foot prosthesis improves walking metabolic economy. *IEEE Trans Robot* 25(1):51–66
38. BiOM (2013) Personal bionics <http://www.biom.com/>
39. Eilenberg MF, Geyer H, Herr H (2010) Control of a powered ankle-foot prosthesis based on a neuromuscular model. *IEEE Trans Neural Syst Rehabil Eng* 18(2):164–173
40. Bionic Technology with Powered Plantar Flexion (2012) <http://www.iwalkpro.com/Prosthetists.html>

41. The technology behind the PROPRIO FOOT® from Össur (2012) <http://www.ossur.com/?PageID=15736>
42. Endolite, élan (2012) <http://www.endolite.com/products/elan>
43. Au SK, Herr H, Weber J, Martinez-Villalpando EC (2007) Powered ankle-foot prosthesis for the improvement of amputee ambulation. In: International conference of the IEEE, Engineering in Medicine and Biology Society, Lyon
44. Herr HM, Grabowski AM (2012) Bionic ankle-foot prosthesis normalizes walking gait for persons with leg amputation. *Proc Biol Sci* 279(1728):457–464. doi:10.1098/rspb.2011.1194
45. Grabowski AM, D'Andrea S (2013) Effects of a powered ankle-foot prosthesis on kinetic loading of the unaffected leg during level-ground walking. *J NeuroEng Rehabil* 10(1):49
46. Gailey R, Allen K, Castles J, Kucharik J, Roeder M (2008) Review of secondary physical conditions associated with lower-limb amputation and long-term prosthesis use. *J Rehabil Res Dev* 45(1):15–30
47. Harlaar J, Becher J, Snijders C, Lankhorst G (2000) Passive stiffness characteristics of ankle plantar flexors in hemiplegia. *Clin Biomech* 15(4):261–270
48. Singer B, Dunne J, Singer K, Allison G (2002) Evaluation of triceps surae muscle length and resistance to passive lengthening in patients with acquired brain injury. *Clin Biomech* 17(2):151–161
49. Chung SG, Rey E, Bai Z, Roth EJ, Zhang L-Q (2004) Biomechanic changes in passive properties of hemiplegic ankles with spastic hypertonia. *Arch Phys Med Rehabil* 85(10):1638–1646
50. Rydahl SJ, Brouwer BJ (2004) Ankle stiffness and tissue compliance in stroke survivors: a validation of myotonometer measurements. *Arch Phys Med Rehabil* 85(10):1631–1637
51. Kobayashi T, Leung AKL, Akazawa Y, Tanaka M, Hutchins SW (2010) Quantitative measurements of spastic ankle joint stiffness using a manual device: a preliminary study. *J Biomech* 43(9):1831–1834
52. Lamontagne A, Malouin F, Richards CL (1997) Viscoelastic behavior of plantar flexor muscle-tendon unit at rest. *J Orthop Sports Phys Ther* 26(5):244–252
53. Hunter IW, Kearney RE (1982) Dynamics of human ankle stiffness: variation with mean ankle torque. *J Biomech* 15(10):742–752
54. Kearney RE, Hunter IW (1982) Dynamics of human ankle stiffness: variation with displacement amplitude. *J Biomech* 15(10):753–756
55. Kearney RE, Hunter IW (1990) System identification of stretch reflex dynamics. *Crit Rev Biomed Eng* 18:55–87
56. Weiss PL, Kearney RE, Hunter IW (1986) Position dependence of ankle joint dynamics—I. Passive mechanics. *J Biomech* 19(9):727–735
57. Weiss PL, Kearney RE, Hunter IW (1986) Position dependence of ankle joint dynamics—II. Active mechanics. *J Biomech* 19(9):737–751
58. Kearney RE, Stein RB, Parameswaran L (1997) Identification of intrinsic and reflex contributions to human ankle stiffness dynamics. *IEEE Trans Biomed Eng* 44(6):493–504
59. Kirsch RF, Kearney RE (1997) Identification of time-varying stiffness dynamics of the human ankle joint during an imposed movement. *Exp Brain Res* 114:71–85
60. Mirbagheri MM, Kearney RE, Barbeau H (1996) Quantitative, objective measurement of ankle dynamic stiffness: intra-subject reliability and intersubject variability. In: 18th annual international conference of the IEEE Engineering in Medicine and Biology Society, Amsterdam
61. Sinkjaer T, Toft E, Andreassen S, Hornemann BC (1998) Muscle stiffness in human ankle dorsiflexors: intrinsic and reflex components. *J Neurophysiol* 60(3):1110–1121
62. Roy A, Krebs HI, Williams DJ, Bever CT, Forrester LW, Macko RM, Hogan N (2009) Robot-aided neurorehabilitation: a novel robot for ankle rehabilitation. *IEEE Trans Robot Automation* 25(3):569–582
63. Saripalli A, Wilson S (2005) Dynamic ankle stability and ankle orientation. 7th symposium on footwear biomechanics conference, Cleveland, OH
64. Zinder SM, Granata KP, Padua DA, Gansneder BM (2007) Validity and reliability of a new in vivo ankle stiffness measurement device. *J Biomech* 40:463–467

65. Fitzpatrick RC, Taylor JL, McCloskey DI (1992) Ankle stiffness of standing humans in response to imperceptible perturbation: reflex and task-dependent components. *J Physiol* 454:533–547
66. Loram ID, Lakie M (2002) Human balancing of an inverted pendulum: position control by small, ballistic-like, throw and catch movements. *J Physiol* 540(3):1111–1124
67. Loram ID, Lakie M (2002) Direct measurement of human ankle stiffness during quiet standing: the intrinsic mechanical stiffness is insufficient for stability. *J Physiol* 545(3):1041–1053
68. Sasagawa S, Ushiyama J, Masani K, Kouzaki M, Kanehisa H (2009) Balance control under different passive contributions of the ankle extensors: quiet standing on inclined surfaces. *Exp Brain Res* 196(4):537–544
69. Winter DA, Patla AE, Rietdyk S, Ishac MG (2001) Ankle muscle stiffness in the control of balance during quiet standing. *J Neurophysiol* 85(6):2630–2633
70. Morasso PG, Sanguineti V (2002) Ankle muscle stiffness alone cannot stabilize balance during quiet standing. *J Neurophysiol* 88(4):2157–2162
71. Shamaei K, Sawicki GS, Dollar AM (2013) Estimation of quasi-stiffness and propulsive work of the human ankle in the stance phase of walking. *PLoS One* 8(3):e59935. doi:[10.1371/journal.pone.0059935](https://doi.org/10.1371/journal.pone.0059935)
72. Farley CT, Blickhan R, Saito J, Taylor CR (1991) Hopping frequency in humans: a test of how springs set stride frequency in bouncing gaits. *J Appl Physiol* 71:2127–2132
73. Farley CT, González O (1996) Leg stiffness and stride frequency in human running. *J Biomech* 29(2):181–186
74. Rouse EJ, Hargrove LJ, Peshkin MA, Kuiken TA (2011) Design and validation of a platform robot for determination of ankle impedance during ambulation. In: Conference proceedings of the IEEE Engineering in Medicine and Biology Society. Boston, MA, USA
75. Rouse E, Hargrove L, Perreault E, Kuiken T (2012) Estimation of human ankle impedance during walking using the Perturberator Robot. Paper presented at the fourth IEEE RAS/EMBS international conference on biomedical robotics and biomechanics, Roma, Italy
76. Rouse E, Hargrove L, Perreault E, Peshkin M, Kuiken T (2013) Development of a robotic platform and validation of methods for estimating ankle impedance during the stance phase of walking. *J Biomech Eng* 135(8):1009-1–1009-8
77. Arndt A, Wolf P, Liu A, Nester C, Stacoff A, Jones R, Lundgren P, Lundberg A (2007) Intrinsic foot kinematics measured in vivo during the stance phase of slow running. *J Biomech* 40:2672–2678
78. Rastgaar M, Ho P, Lee H, Krebs HI, Hogan N (2009) Stochastic estimation of multi-variable human ankle mechanical impedance. In: ASME dynamic systems and control conference, Hollywood, CA
79. Rastgaar M, Ho P, Lee H, Krebs HI, Hogan N (2010) Stochastic estimation of the multi-variable mechanical impedance of the human ankle with active muscles. In: ASME dynamic systems and control conference, Boston, MA
80. Lee H, Ho P, Krebs HI, Hogan N (2009) The multi-variable torque-displacement relation at the ankle. In: ASME dynamic systems and control conference, Hollywood, CA
81. Lee H, Ho P, Rastgaar M, Krebs HI, Hogan N (2010) Quantitative characterization of steady-state ankle impedance with muscle activation. In: ASME dynamic systems and control conference, Cambridge, MA
82. Lee H, Ho P, Rastgaar M, Krebs HI, Hogan N (2011) Multivariable static ankle mechanical impedance with relaxed muscles. *J Biomech* 44:1901–1908
83. Lee H, Ho P, Rastgaar M, Krebs HI, Hogan N (2014) Multivariable static ankle mechanical impedance with active muscles. *IEEE Trans Neural Syst Rehabil Eng* 22(1):44–52
84. Ho P, Lee H, Krebs HI, Hogan N (2009) Directional variation of active and passive ankle static impedance. Paper presented at the ASME dynamic systems and control conference, Hollywood, CA
85. Ho P, Lee H, Rastgaar M, Krebs HI, Hogan N (2010) The interpretation of the directional properties of voluntarily modulated human ankle impedance. In: ASME dynamic systems and control conference, Cambridge, MA

86. Lee H, Krebs HI, Hogan N (2012) Linear time-varying identification of ankle mechanical impedance during human walking. In: ASME 2012 5th annual dynamic systems and control conference, Fort Lauderdale, FL, USA
87. Taylor MJD, Dabnichki P, Strike SC (2005) A three-dimensional biomechanical comparison between turning strategies during the stance phase of walking. *Hum Mov Sci* 24:558–573
88. A Roadmap for US Robotics, From Internet to Robotics. (Computing Community Consortium, May 21, 2009). <http://www.us-robotics.us/reports/CCC%20Report.pdf>
89. Ficanha EM, Rastgaar M, Modirian B, Mahmoudian N (2013) Ankle Angles during Step Turn and Straight Walk: implications for the design of a steerable ankle-foot Prosthetic Robot. In: Dynamic systems and controls conference Stanford University, Palo Alto, CA